SOILS AND FOUNDATIONS Vol. 29, No. 4, 127-134, Dec. 1989
Japanese Society of Soil Mechanics and Foundation Engineering

TECHNICAL NOTE

DISTRIBUTION OF GROUTS IN SOLIDIFIED REGION ON CHEMICAL GROUTING

Akira Mori[i], Masahito Tamura[ii] and Yoshihiro Fukui[iii]

ABSTRACT

This paper investigates the volume ratio α of grout entered into void space in each part of solidified region by chemical grouting for the sandy ground. In long gel time grouts, the value of α is in 80~100% unless the hydrofracturing occurs and α does not practically depend on the distance from the injection borehole. On the other hand, in short gel time grouts, α of the region near to injection hole is more than 100%, because the pore gel in the solidified body is concentrated when the succeeding grouts penetrate the solidified body. As a whole, the solidified volume is almost equal to the solidified volume when α is supposed to be 100%, irrespective of the gel time of grouts, as long as the injection rate q is smaller than the critical injection rate q_{CR}. q_{CR} is the maximum value of injection rate which does not initiate the hydrofracturing of ground.

Key words : grouting, permeability, sandy soil, soil stabilization, volume ratio of grout entered in the void, unconfined compression test (**IGC** : K 6/E 7)

INTRODUCTION

Grouting is a convenient method to control the groundwater and to strengthen the ground in excavation. However, the grouting theory to solidify the desired region has not been established yet. Therefore, it is necessary to clarify the relation between the solidified region and the grouting condition, for example, the injection volume, the injection rate, and the gel time of grouts. It is especially important to estimate the quality of solidified region and the solidified shape, because the decision of total injection volume is deeply related to the uniformity of the solidified region.

The volume ratio α of grout entered into the void space of each part in sandy ground is a reliable index to estimate the uniformity of solidified region. Kawachi and Kita

i) Professor, Department of Civil Engineering, Waseda University, Shinjuku-ku, Tokyo.
ii) Research Engineer, Geotechnical Engineering Division, Building Research Institute, Ministry of Construction, Tsukuba, Ibaraki.
iii) Graduate Student, Waseda University, Shinjuku-ku, Tokyo.
Manuscript was received for review on January 20, 1989.
Written discussions on this note should be submitted before July 1, 1990, to the Japanese Society of Soil Mechanics and Foundation Engineering, Sugayama Bldg. 4 F, Kanda Awaji-cho 2-23, Chiyoda-ku, Tokyo 101, Japan. Upon request the closing date may be extended one month.

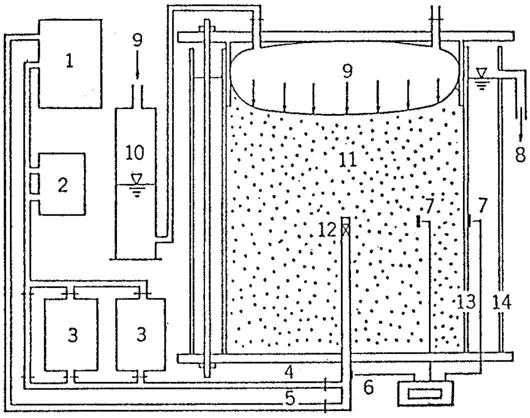

Fig. 1. Schematic diagram of injection apparatus

(1985, 1987) had reported the relation between the grouting method and the distribution of grouting mateial. However, little is known about the effects of gel time G_t, injection rate q, and injection pressure P' on the ratio α.

The purpose of this study is to clarify the relation between the ratio α and some grouting conditions. In experiments, the injection tests using several kinds of sands and three different gel time of grouts were performed.

TEST PROCEDURE AND SAMPLES

Fig. 1 shows the grouting apparatus with the injection pump. Size of the test specimen was 80 cm both in diameter and height. The sand was packed into the inner cylinder, which was made of the porous steel, and was compacted in the desired density. The outer cylinder was made of lucite of which diameter was 100 cm. The outer cylinder was filled with water. And the specimen was saturated with water. The injection rate q was measured by the electro-magnetic flow meter.

The overburden pressure σ_v was given by expanding the rubber balloon fixed to the upper board of inner cylinder.

Table 1. Types of sands

Sample	Void ratio e	Coefficient of permeability k (cm/sec)	Frictional angle ϕ' (°)
A	1.09	1.1×10^{0}	34.7
B	0.88	1.3×10^{-1}	34.3
C	1.00	5.3×10^{-2}	34.8
D	1.00	2.0×10^{-2}	33.4
E	1.00	5.1×10^{-3}	38.1
F	1.00	1.6×10^{-3}	38.1
G	1.00	2.4×10^{-3}	36.1
H	1.00	7.8×10^{-4}	37.6

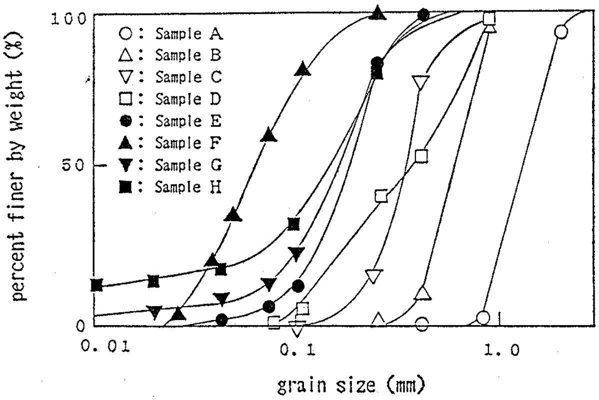

Fig. 2. Grain size distribution curves

Table 2. Used chemical grouts

Type	Content		Gel time G_t
	Liquid A (500 cc)	Liquid B (500 cc)	
a short gel time	Water glass 250 cc Water 250 cc	Glyoxal 50 cc Phosphoric acid 25 cc Water 425 cc	5~10 (sec)
b middle gel time	Water glass 250 cc Water 250 cc	Glyoxal 50 cc Phosphoric acid 15 cc Water 435 cc	50~70 (sec)
c long gel time	Water glass 250 cc Water 250 cc	Glyoxal 50 cc Phosphoric acid 8 cc Water 442 cc	20~30 (min)

Table 1 shows the physical properties of samples. Fig. 2 shows the grain size distribution curves.

Table 2 shows the combination of grout components and the gel time G_t. The hardeners were glyoxal ($(CHO)_2$) and phosphoric acid (H_3PO_4). The liquid A shown in Fig. 1 was 50% water glass. Glyoxal ($(CHO)_2$) and phosphoric acid (H_3PO_4) were contained in the liquid B. They were mixed in the top of injection pipes. Liquid A and B were injected into the specimen with the same volume. The total injection volume Q was $50\,l$ in all cases.

After the injection, the specimen was left for 24 hours, and then soil samples were cut down from the solidified mass and the volume ratio α of grout entered into the void as well as the unconfined compressive strength q_u of solidified sand were measured. The value of α is given by Eq. (1).

$$\alpha(\%)=\frac{(a_2-a_3)\cdot 100}{a_1\cdot(n/100)} \qquad (1)$$

α : volume ratio of grout entered in the void space (%)
a_1 : silica content of grout (mg/cc)
a_2 : dissolved silica content of soil sample after injection (mg/cc)
a_1 : dissolved silica content of soil sample before injection (mg/cc)
n : porosity (%)

The volume ratio α of grout entered into the void space was determined by the weight of dissolved silica contained in soil samples. The dissolved silica was extracted from the solidified parts by sodium hydroxide (Hashimoto and Jackson, 1960) and the weight was determined by the atomic absorption analysis.

LONG GEL TIME GROUTS

In using long gel time grouts, of which gel time is longer than the injection time, the solidified shape deeply depends upon the injection rate q. The authors had demonstrated that the grouts could permeate without fracturing as long as the injection rate q was smaller than the critical injection rate q_{CR} (Mori, Tamura and Hirano, 1987). If q is smaller than q_{CR}, the injection pressure P' increases as q increases. However, P' decreases as q increases if q exceeds q_{CR}.

Fig. 3 shows the relation between the injection pressure P' using the water instead of grouts and the injection rate q.

$$P'=P-R_P \qquad (2)$$

P : borehole pressure
R_P : resistant pressure

The resistant pressure R_P was the sum of the initial pore water pressure and the resistance of injection liquid flowing out through the injection pipe.

It was found from Fig. 3 that except the case of sample H, the spherical permeation from the injection borehole was possible, because q did not reach to q_{CR} (Mori, Tamura and Haraguchi, 1989).

Fig. 4 shows the relation between the value of α in solidified parts and the distance D from the injection borehole. The solidified parts were not broken when the water poured to the specimen after the injection test. The value of α was not practically influenced by D and was 80~100% in the solidified parts, except sample H and G. And α remarkably decreased in the boundaries between the solidified and the unsolidified parts. The value of α of unsolidified parts was much smaller than that of solidified parts.

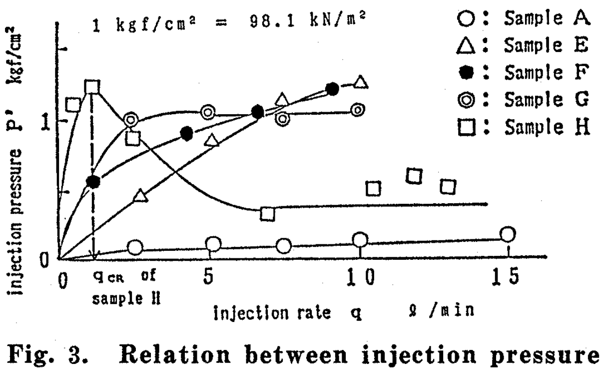

Fig. 3. Relation between injection pressure P' and injection rate q

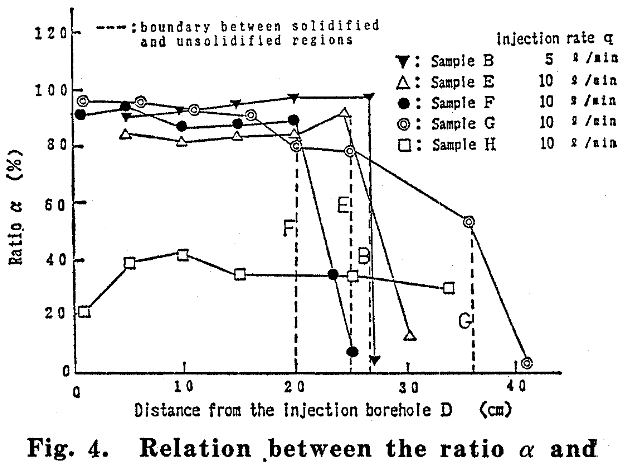

Fig. 4. Relation between the ratio α and the distance D from the injection borehole by long gel time grout

In sample H, α was small even in the solidified parts. In this case, hydrofracturing occurred and some laminar gels were formed along the fracturing surface. Although the soil sandwiched by the gels was solidified in a mass, the grouts did not fully permeate. This is probably because α of sample H was small as compared with other sands. In sample G, 10 l/min of q was nearly equal to q_{CR}, for the inclination of $P'\sim q$ curve was almost 0° (cf. Fig. 3). This fact means that the grouts penetrated into soils with fracturing to some degree. For that reason, α of sample G would have been small.

The solidified shapes were almost spherical and simple mass except in the case of sample H. The solidified shape of sample H was laminar. In this case, the most parts of injection grouts flow out of the specimen along the fracturing surface. And the ratio α is not related to the distance from the borehole, but to that from the fracturing surface. Therefore it is concluded that the ratio α depends upon the existence of hydrofracturing phenomenon by injection grouts and the value of solidified part was 80~100% as long as the injection rate q is smaller than the critical injection rate q_{CR}. If q is larger than q_{CR}, the grouts penetrate into the soils with fracturing and flow out of the desired region.

In addition, in sample A, of which permeability was 1 cm/s, the solidified region around the injection borehole was not seen at all, because grouts went down due to the difference of specific gravity between the grouts and the pore water. And so it should be noted that the long gel time grouts are not suitable for the grounds of high permeability.

Fig. 5 shows the relation between the distance D from the injection borehole and the unconfined compressive strength q_u. The dashed lines in Fig. 5 indicate q_{uO} of artificially prepared "sand-gel" specimen, which was mixed with sand and grout in the mold of which diameter was 5 cm. α of "sand-gel" is almost equal to 100%. q_u of solidified

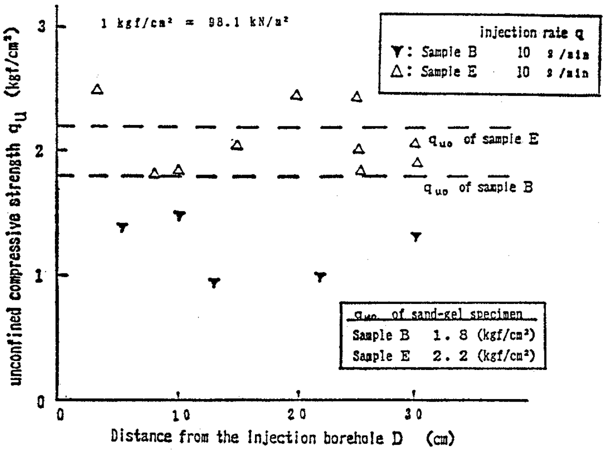

Fig. 5. Relation between the distance D from the injection borehole and unconfined compressive strength q_u by long gel time grout

sands by injection was a little smaller than q_{uO}, because α of solidified sands was smaller than 100%.

The relation between the ratio α and the distance D from the borehole can be deduced from the convective dispersion equation in three dimensions shown by Eq. (3). The dispersion coefficient D_c is supposed to be given by Eq. (4) (Harleman, Mehlhorn and Rumer, 1963).

$$\frac{\delta S}{\delta t}+u\frac{\delta S}{\delta r}=D_c\left(\frac{\delta^2 S}{\delta r^2}+\frac{2}{r}\cdot\frac{\delta S}{\delta r}\right) \quad (3)$$

$$\frac{D_c}{\nu}=88\cdot R_k{}^{1.2} \quad (4)$$

$$R_k=\frac{|u|k^{0.5}}{\nu} \quad (5)$$

D_c : dispersion coefficient (cm²/s)
R_k : permeability Reynolds number
S : concentration
r : coordinate direction (cm)
ν : kinematic viscosity (cm²/s)
k : coefficient of permeability (cm/s)
u : seepage velocity (=U/n) (cm/s)
U : superficial velocity (cm/s)
n : porosity t : time (s)

α $(=(S/S_0)\times 100$, S_0 : initial concentration of grouts) in Fig. 6 was the value calculated by Eq. (4) using the finite difference method. The injection rate q was 10 l/min in both cases. The injection time t of case

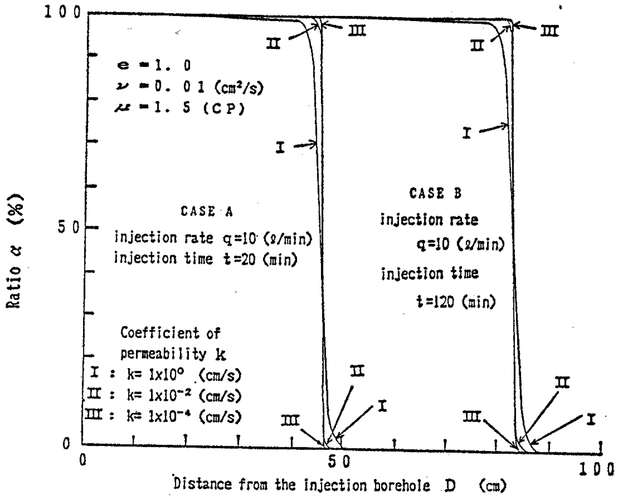

Fig. 6. Relation between the value α and D by convective dispersion equation

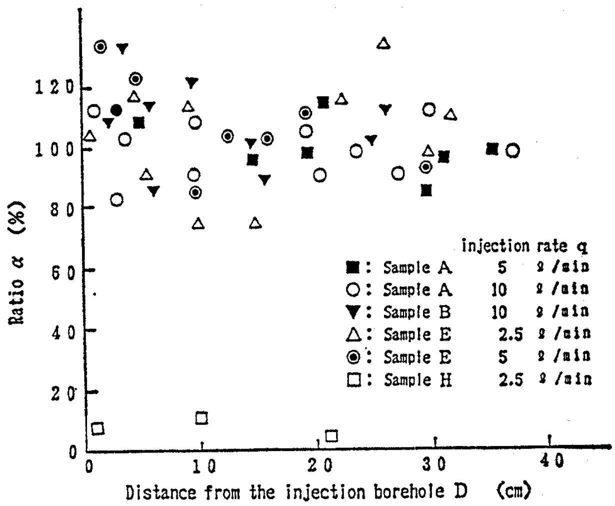

Fig. 7. Relation between the ratio α and the distance D from the injection borehole by short gel time grout

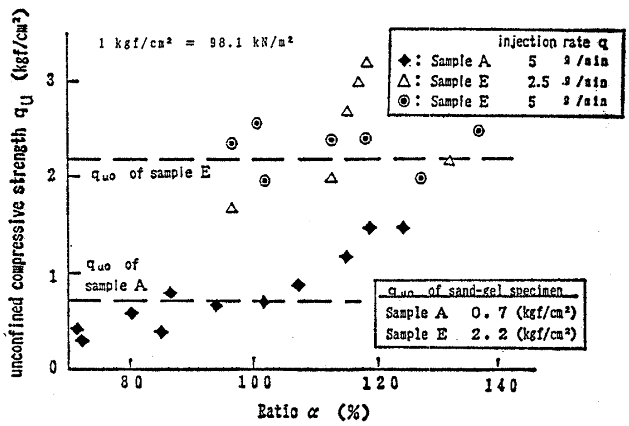

Fig. 8. Relation between the ratio α and unconfined compressive strength q_u by short gel time grout

A was 20 min and that of case B 120 min. Supposed that the grouts perfectly permeated into the ground in 100% of α, the distance D_t of permeation by grouts in case A was 43.5 cm and that in case B was 85 cm, respectively. It was found from Fig. 6 that α' abruptly decreased at D_t and the grouts hardly diffused during injection.

The values of α in these tests seemed to be a little larger than α of in-situ solidified sands measured by Kawachi and Kita (1987). In sandy samples used here, the ratio of free water to the total pore water is probably larger than that in the case of field, because the grain size of sandy samples is comparatively uniform. If the grain size is uniform, the ratio of free water is large and the most part of pore water can be replaced by the grouts (Chida, 1982). On the other hand, in the field the replacement of grouts does not fully occur even if the grouts permeate without fracturing because the ratio of free water in in-situ sands was small. For that reason, α of in-situ solidified sands would be small as compared with the results as shown here. However, the diffusion of grouts probably does not occur even in the real grounds.

SHORT GEL TIME GROUTS

In short gel time grouts, of which gel time is shorter than the injection time t, the succeeding grouts cannot be injected unless the parts solidified by the preceding grouts are fractured or perforated.

Fig. 7 shows the relation between α and D by short gel time grouts. The value of α seemed to be larger than that in the case of long gel time grouts. It exceeded 100% in some cases and α tended to exceed 100% near the injection borehole.

Fig. 8 shows the relation between α and q_u. In several cases, q_u was larger than q_{u0} of "sand-gel" specimen of which α was 100%, because α of these cases exceeded 100%.

Table 3. Effect of overburden pressure on the ratio α
cf. Sample E, short gel time grout q=10(l/min)

σ_v(kgf/cm²)	D(cm)	α(%)	q_u(kgf/cm²)
3	0	130	6.32
	10	132	5.12
	20	112	3.44
	30	108	3.83
1	0	118	3.20
	10	102	2.61
	20	98	1.78
	30	103	2.07

1 kgf/cm²=98.1 kN/m²

σ_v : overburden pressure
D : distance from the injection borehole
α : volume ratio of grout entered in the void
q_u : unconfined compressive strength

The authors had pointed out that the solidified shapes by short gel time grouts depended upon the degree of permeation in the "perforating stage" (Mori et al., 1988). After the injection time elapsed about the gel time, the succeeding grouts permeated with perforating the solidified parts by the preceding grouts. In this stage, the grouts permeated in radial direction through the solidified zone from the borehole and the solidified shape grew up spherically until the hydrofracturing occurs.

The hydrofracturing is difficult to occur as the permeability or the confining pressure increases. It is because the hydrofracturing pressure P_f' becomes larger as the permeability as well as the confining pressure become larger (Mori, Tamura and Chun, 1987; Mori and Tamura, 1987). For that reason, the perforating stage continues in longer term in the case of high permeability or high confining pressure.

The reason why α in short gel time grouts exceeded 100% is probably resulted from the consolidation of pore gel by the successive grouts. In the perforating stage, the water in pore gel would be pushed away by the succeeding grouts and then concentrated.

Table 3 shows the effect of overburden pressure σ_v on α. The value of α increased as σ_v increased, because the hydrofracturing was difficult to be generated and the perforating stage continued in longer term as σ_v increased. The unconfined compressive strength q_u in σ_v=3.0 kgf/cm² (294 kN/m²) was much larger than that in σ_v=1.0 kgf/cm²

Table 4. Relation between the ratio α and unconfined compressive strength q_u of in-situ solidified sand by short gel time grout

	α(%)	q_u(kgf/cm²)
fine sand	122.2	13.8
	131.1	11.9
coarse sand	110.2	4.86
	79.5	1.40
	82.2	1.20
	75.5	1.35
	76.2	1.70
	115.7	7.50

1 kgf/cm²=98.1 kN/m²

q_{u0} of sand-gel specimen prepared in the mold (α=100%)
fine sand =5.0(kgf/cm³)
coarse sand=4.0(kgf/cm²)

Table 5. Solidified shape and solidified ratio R_s

Sample	q (l/min)	σ_v (kgf/cm²)	gel time	Shape	W (kgf)	R_s (%)
A	2.5	1	short	◎	204	109
A	10	1	short	◎	177	101
A	10	1	long	—	—	—※
C	10	1	short	○	196	107
C	10	3	short	◎	165	87
C	10	1	middle	○	180	96
D	10	1	short	○	217	105
D	10	1	long	◎	211	103
D	10	3	short	◎	173	85
E	2.5	1	short	△	181	102
E	10	1	short	△	181	105
E	10	3	short	○	172	87
E	10	1	middle	○	215	115
E	10	1	long	◎	220	120
F	10	1	long	○	212	116
G	10	1	short	△	192	92
G	10	1	middle	○	193	94
G	10	1	long	◎	220	115
H	2.5	1	short	×	12	7
H	2.5	1	long	×	112	55
H	10	1	long	×	92	52

1 kgf/cm²=98.1 kN/m²

◎ : spherical
○ : intermediate between spherical and plank
△ : plank
× : The solidified parts did not exist due to hydrofracturing occurred.
※ : The entered grouts went down before gelling, because grouts went down due to the difference of specific gravity between grouts and pore water.

($98\,kN/m^2$), because α of the former was larger. For this reason, when grouts of short gel time are used and overburden pressure σ_v is large, i.e. in the case of grouting in large depth, the average α is more than 100% and the unconfined compressive strength q_u, as a whole, becomes larger.

Table 4 shows the relation between α and q_u of in-situ solidified sands. The concentration of gel was confirmed in the field as well as in the laboratory. q_u of solidified sands with α exceeded 100% by field injection was much larger than q_{u0} of "sand-gel" specimen that was made of the field sand and the grout.

SHAPE AND VOLUME OF THE SOLIDIFIED REGION

Table 5 shows the relationship between the solidified shape and solidified volume ratio R_s given by Eq. (6).

$$R_s(\%)=\frac{V_s\cdot 100}{V_{s100}} \qquad (6)$$

$$=\frac{n\cdot W_s}{\rho\cdot Q} \qquad (7)$$

V_S : solidified volume (l)
V_{S100} : theoretical solidified volume when the total injection grouts permeate in 100% of α. (l)
W_S : solidified weight (kgf)
Q : total injection grout volume (l)
n : porosity (%)
ρ : density (g/cm^3)

The solidified shapes were classified into four types as shown in Table 5. To our surprise, the spherical solidified body was seen not only in long gel time grouts but also short gel time grouts. In the sand of which permeability is very high, the short gel time grouts is recommended rather than the long gel time grouts, becuase the sedimentation of grouts occurs in long gel time grouts.

R_S of sample H was fairy small since the loss of grouts caused by the hydrofacturing was remarkably large. In respect of gel time, R_s by short gel time grouts seemed to be a little smaller than R_s by long gel time grouts because of the concentration phenomenon of grouts resulted from the perforation of pore gels. However, as a whole, it can be concluded that R_s is about 100% irrespective of gel time as long as the injection rate q is smaller than q_{CR}. If q is smaller than q_{CR}, the hydrofracturing could not be generated in the unsolidified parts, irrespective of gel time.

In respect of overburden pressure σ_v, the solidified shape became more spherical as σ_v became larger. And R_s of short gel time grouts in $\sigma_v=3.0\,kgf/cm^2$ ($294\,kN/m^2$) was smaller than that in the case of $\sigma_v=1.0\,kgf/cm^2$ ($98\,kN/m^2$). This is probably due to the fact that the concentration of pore gels in the former case becomes high degree.

CONCLUSIONS

The value α by short gel time grouts is generally larger than that by long gel time grouts and is larger than 100% in some cases. This phenomenon is resulted from the concentration of pore gels in the perforating stage. In this stage, the grouts permeate uniformly and spherically, pushing away the pore gels.

In the case when injection rate q is smaller than critical injection rate q_{CR}, i.e. under the condition that hydrofracturing does not occur in unsolidified parts, the value of α by long gel time grouts is always 80~100% and does not depend on the distance from the borehole.

As a whole, the solidified ratio R_s given by Eq. (6) is about 100%, irrespective of gel time of grouts as long as the injection rate q is smaller than the critical injection rate q_{CR}. If q is larger than q_{CR}, the hydrofracturing occurs in the unsolidified parts, irrespective of gel time and the loss of grouts is large.

REFERENCES

1) Kawachi, T. and Kita, T. (1985): "Study on performance control of chemical grouting (Part 5)," Report of the Technical Research Institute OHBAYASHI CORPORATION, No.

30, pp. 117–122 (in Japanese).
2) Kawachi, T. and Kita, T. (1987) : "Investigation for the distribution of grouted material and ground improvement effect," Tsuchi-to-Kiso, JSSMFE, No. 352, Vol. 35, No. 5, pp. 45–50.
3) Hashimoto, I. and Jackson, M. L. (1960) : "Rapid dissolution of allophane and kaolinite-halloysite after dehydration," 17 th National Conference on Clay and Clay Minerals, pp. 102–113.
4) Mori, A., Tamura, M. and Hirano, M. (1987) : "The injected shapes by long gel time grouts and the governing condition," JSCE, No. 388, pp. 131–140 (in Japanese).
5) Harleman, D. R. F., Mehlhorn, P. F. and Rumer, R. R. (1963) : "Dispersion-permeability correlation in porous media," Proc. ASCE, Vol. 89, No. HY 2, pp. 67–85.
6) Mori, A., Tamura, M. and Haraguchi, K. (1989): "Solidified shapes by short gel time grouts in sandy ground and the governing condition," JSCE, (to be published).
7) Mori, A., Tamura, M., Haraguchi, K. and Satoh, Y. (1988) : "Relation between solidified shape and gel time on chemical grouting," Proc. 23 rd Annual Meeting of JSSMFE, pp. 2093–2100 (in Japanese).
8) Mori, A., Tamura, M. and Chun, B. (1987) : "Mechanism of hydraulic fracturing in sandy soils," JSCE, No. 388, pp. 61–70 (in Japanese).
9) Mori, A. and Tamura, M. (1987) : "Hydrofracturing phenomena in soil ground," Memoirs of the School of Science & Engineering, Waseda University, No. 51, pp. 33–60.
10) Chida, S. (1982) : Method of Improvement on Soft Ground, Kajima Shuppankai Co., Ltd., pp. 163–165 (in Japanese).